

Decay analysis of compound nuclei $^{194}\text{Hg}^*$, $^{200}\text{Pb}^*$, $^{203}\text{Bi}^*$ and $^{207}\text{At}^*$ within dynamical cluster decay model

Sarbjeet Kaur^{1,2,*}, BirBikram Singh^{2,†} and S.K. Patra^{3,4}

¹Department of Physics, Sri Guru Granth Sahib World University, Fatehgarh Sahib-140406, India

²Department of Physics, Akal University, Talwandi Sabo-151302, India

³Institute Of Physics, Sachivalya Marg, Bhubhaneswar-751005, India and

⁴Homi Bhabha National Institute, Anushakti Nagar, Mumbai - 400094, India

Introduction

The neutron deficient nuclei lying close to the proton drip line are more difficult to populate in their excited states and they can be produced in fusion-evaporation reactions with stable heavy-ion beams and stable targets [1]. With the advancement in ion-beam facility the exploration of the properties of nuclei towards drip-lines has become possible. In present study, we explore the decay of exotic neutron deficient nuclei $^{194}\text{Hg}^*$, $^{200}\text{Pb}^*$, $^{203}\text{Bi}^*$ and $^{207}\text{At}^*$ formed in ^{19}F induced reactions on the targets ^{175}Lu , ^{181}Ta , ^{184}W and ^{188}Os , respectively.

Recent studies observe that in drip-line regions there is disappearance of some traditional magic numbers (specific proton or neutron numbers that give additional stability to the nucleus) and appearance of the new magic numbers in the light mass nuclei [2]. It is interesting to explore magicity effects in the heavier mass regions of the nuclear landscape. In previous study the effect of neutron shell closures $N = 126$, had been explored to investigate the decay of compound nuclei (CN) [3], within the quantum mechanical fragmentation theory based Dynamical Cluster Decay Model (DCM) [3, 4]. The study revealed that the most prominent fusion-fission fragments for the decay of CN under study are having neutron-proton counts closer to the magic numbers. In present study we shifted to $N \leq 126$ and $Z \sim 82$ i.e. below and above the proton shell closure $Z = 82$ region and further

explored the effect of increase in temperature on the $Z = 82$ proton shell closure. We have calculated the σ_{ERs} for all the four reactions at extreme E_{lab} values, leading to CN with $A \sim 200$, in reference to the available experimental data [5].

Methodology

The DCM is worked out in terms of collective coordinates of relative separation R , with deformations β_2 and orientations θ_i of two fragments ($i = 1, 2$) and mass asymmetry $\eta_A = (A_1 - A_2)/(A_1 + A_2)$. In terms of these coordinates, the compound nucleus (CN) decay cross-section for ℓ - partial waves, is defined as

$$\sigma = \frac{\pi}{k^2} \sum_{\ell=0}^{\ell_{max}} (2\ell + 1) P_0 P; \quad k = \sqrt{\frac{2\mu E_{c.m.}}{\hbar^2}} \quad (1)$$

where, P_0 is preformation probability obtained by solving the stationary Schrödinger equation and P , the barrier penetrability, calculated as the WKB tunneling probability, both dependent on T and ℓ . The reduced mass $\mu = [A_1 A_2 / (A_1 + A_2)]$ and ℓ_{max} is the maximum angular momentum. The ℓ_{max} is fixed for vanishing LPs/ERs cross-section (σ_{ERs}), i.e., $\sigma_{ERs} \rightarrow 0$.

Calculations and Discussion

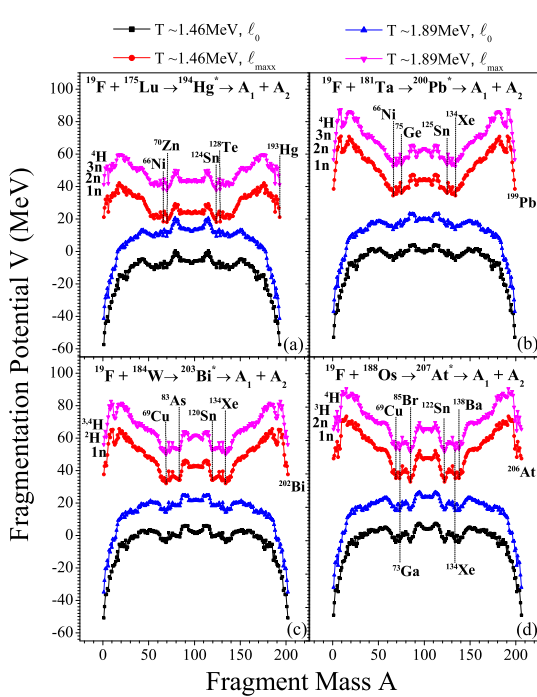
Fig. 1(a-d) presents the potential energy surface or fragmentation potential V (MeV) of the favored fragments, for the decay of CN $^{194}\text{Hg}^*$, $^{200}\text{Pb}^*$, $^{203}\text{Bi}^*$ and $^{207}\text{At}^*$, respectively, at extreme T -values. As we move from Fig. 1(a) to Fig. 1(d) we observe interplay between LPs and fission fragments, specifically at higher ℓ -values. The LPs which are strongly minimized at $\ell = 0\hbar$ value, are almost superseded by fission fragments at the respective

*Electronic address: sarbjeetsangha13@gmail.com

†Electronic address: bir_phy@auts.ac.in

TABLE I: DCM calculated σ_{ERs} for the compound nuclei presented in Fig. 1 and their comparison with the experimental data [5].

Compound Nucleus Decay	E_{lab} (MeV)	$E_{c.m.}$ (MeV)	E_{CN}^* (MeV)	Temp. (MeV)	ℓ_{max} (\hbar)	ΔR (fm)	DCM	σ_{ERs} (mb) Expt.
$^{19}\text{F} + ^{175}\text{Lu} \rightarrow ^{194}\text{Hg}^*$	79.000	71.263	46.792	1.496	107	1.647	70.609	69.973
$^{19}\text{F} + ^{181}\text{Ta} \rightarrow ^{200}\text{Pb}^*$	80.194	72.576	48.898	1.506	129	1.450	13.738	13.151
$^{19}\text{F} + ^{184}\text{W} \rightarrow ^{203}\text{Bi}^*$	79.104	71.700	46.029	1.451	125	1.259	0.568	0.5973 ± 1
$^{19}\text{F} + ^{188}\text{Os} \rightarrow ^{207}\text{At}^*$	79.397	72.109	42.710	1.386	130	1.333	0.663	0.661
$^{19}\text{F} + ^{175}\text{Lu} \rightarrow ^{194}\text{Hg}^*$	115.686	104.356	79.888	1.948	110	1.945	554.984	551.289 ± 32.95
$^{19}\text{F} + ^{181}\text{Ta} \rightarrow ^{200}\text{Pb}^*$	114.349	103.165	79.176	1.901	131	1.831	444.725	444.335
$^{19}\text{F} + ^{184}\text{W} \rightarrow ^{203}\text{Bi}^*$	114.258	103.564	77.893	1.880	127	1.749	207.767	204.4 ± 36.8
$^{19}\text{F} + ^{188}\text{Os} \rightarrow ^{207}\text{At}^*$	115.000	104.444	75.045	1.828	131	1.738	88.635	88.825


 FIG. 1: The fragmentation potential V (MeV) as a function of fragment mass A at extreme ℓ values for CN (a) $^{194}\text{Hg}^*$ (b) $^{200}\text{Pb}^*$ (c) $^{203}\text{Bi}^*$ (d) $^{207}\text{At}^*$, at $E_{lab} \sim 79$ and 115 MeV.

ℓ_{max} -values (see Table I). Comparatively, we find here that LPs are in competition for the cases of CN $^{194}\text{Hg}^*$, $^{200}\text{Pb}^*$, $^{203}\text{Bi}^*$, even at higher ℓ -values. However, for the case $^{207}\text{At}^*$ fission fragments are quite dominant at higher

ℓ -values. As we go from $T \sim 1.46$ MeV to $T \sim 1.89$ MeV, the magnitude of the fragmentation potential increases but the pattern/behavior of LPs and fission fragments remains same. It is clear from Fig. 1(a-d) by moving to higher temperatures systems becomes exotic as compared to the lower T -values. Further, the given potential energy surfaces of all the CN lead to almost similar preformation probability values at the extreme temperature values. However, subsequent process of scattering of potential barriers yield higher values of penetration probability values for the CN under study, at the extreme temperature values. Consequently, the DCM calculated values of evaporation residue cross-sections σ_{ERs} are large in comparison to the values calculated at lower T -values, which are in good comparison with the experimental data [5], as presented in Table I.

References

- [1] R. Julin, T. Grahn, J. Pakarinen and P. Rauhila, J. Phys. G: Nucl. Part. Phys. **43**, 024004 (2016).
- [2] A. Ozawa, et al., Phys. Rev. Lett. **84**, 5493 (2000).
- [3] R. Kaur, B.B. Singh, et al., Proc. of the DAE Symp. on Nucl. Phys. **62**, 632 (2017).
- [4] S. Kaur, M. Kaur et al., Proc. of the DAE Symp. on Nucl. Phys. **63**, 472 (2018).
- [5] S. Nath, P. V. Madhusudhana Rao, et al., Phys. Rev. C **81**, 064601 (2010).